

Medicago truncatula Yellow Stripe-Like7 encodes a peptide transporter participating in symbiotic nitrogen fixation

Rosario Castro-Rodríguez¹ | Viviana Escudero¹ | María Reguera¹  |
 Patricia Gil-Díez¹ | Julia Quintana²  | Rosa Isabel Prieto¹ | Rakesh K. Kumar³ |
 Ella Brear⁴ | Louis Grillet⁵ | Jiangqi Wen⁶ | Kirankumar S. Mysore⁶  |
 Elsbeth L. Walker³ | Penelope M. C. Smith⁴  | Juan Imperial⁷ |
 Manuel González-Guerrero^{1,8} 

¹Centro de Biotecnología y Genómica de Plantas (UPM-INIA), Universidad Politécnica de Madrid, Campus de Montegancedo, Madrid, Spain

²Department of Chemistry and Biochemistry, Worcester Polytechnic Institute, Worcester, Massachusetts

³Department of Biology, University of Massachusetts, Amherst, Massachusetts

⁴Department of Animal, Plant, and Soil Sciences, La Trobe University, Bundoora, Australia

⁵Department of Agricultural Chemistry, National Taiwan University, Taipei, Taiwan

⁶Noble Research Institute, LLC., Ardmore, Oklahoma

⁷Instituto de Ciencias Agrarias, Consejo Superior de Investigaciones Científicas, Madrid, Spain

⁸Escuela Técnica Superior de Ingeniería Agronómica, Alimentaria y de Biosistemas, Universidad Politécnica de Madrid, Madrid, Spain

Correspondence

Manuel González-Guerrero, Centro de Biotecnología y Genómica de Plantas (UPM-INIA), Universidad Politécnica de Madrid, Campus de Montegancedo. Crta. M-40 km 38. 28223 Pozuelo de Alarcón (Madrid), Spain.
 Email: manuel.gonzalez@upm.es

Funding information

Agencia Estatal de Investigación, Grant/Award Number: SEV-2016-0672; Australian Research Council Industrial Transformation Research Hub, Grant/Award Number: IH140100013; European Research Council, Grant/Award Number: ERC-2013-StG-335284; Ministerio de Economía y Competitividad, Grant/Award Numbers: AGL2015-65866-P, BES-2013-062674; National Science Foundation, Grant/Award Number: DBI-0703285

Abstract

Yellow Stripe-Like (YSL) proteins are a family of plant transporters that are typically involved in transition metal homeostasis. Three of the four YSL clades (I, II and IV) transport metals complexed with the non-proteinogenic amino acid nicotianamine or its derivatives. No such capability has been shown for any member of clade III, but the link between these YSLs and metal homeostasis could be masked by functional redundancy. We studied the role of the clade III YSL protein MtYSL7 in *Medicago truncatula* nodules. MtYSL7, which encodes a plasma membrane-bound protein, is mainly expressed in the pericycle and cortex cells of the root nodules. Yeast complementation assays revealed that MtYSL7 can transport short peptides. *M. truncatula* transposon insertion mutants with decreased expression of MtYSL7 had lower nitrogen fixation rates and showed reduced plant growth whether grown in symbiosis with rhizobia or not. YSL7 mutants accumulated more copper and iron in the nodules, which is likely to result from the increased expression of iron uptake and delivery genes in roots. Taken together, these data suggest that MtYSL7 plays an important role in the transition metal homeostasis of nodules and symbiotic nitrogen fixation.

KEYWORDS

Medicago truncatula, peptide transport, symbiotic nitrogen fixation, YSL

1 | INTRODUCTION

Iron, copper, zinc and other transition metals are essential nutrients for plants (Marschner, 2011). These elements are structural components or cofactors of proteins involved in almost every physiological process. Therefore, the ability to obtain transition metals from the soil and to deliver them to hundreds of metalloproteins in different organelles and tissues is essential for plant development. Several metal transport families participate in transition metal allocation (Kobayashi & Nishizawa, 2012; Olsen & Palmgren, 2014; Pilon, 2011). Although most of them are conserved in all domains of life, a few, such as the Yellow Stripe-Like (YSL) proteins, are exclusively present in plants (Curie et al., 2008; Kumar et al., 2017), suggesting selective pressures for specialized metal transport systems. YSL transport proteins are evolutionarily related to members of the Oligopeptide Transporter (OPT) family, and both share the ability to transport amino acid substrates into the cell cytosol (Lubkowitz, 2011). Biochemically characterized YSLs typically transport the non-proteinogenic amino acid nicotianamine or nicotianamine-derived molecules (mugineic acids) as complexes with transition elements (Aoyama et al., 2009; Schaaf et al., 2004).

The founding member of the YSL family is *Zea mays* YS1. Mutants in this gene present interveinal chlorosis in leaves (yellow stripes), as a result of a deficiency in iron uptake (Beadle, 1929; Curie et al., 2001). ZmYS1 and its orthologues (eg, OsYSL15) are the main iron uptake system from soil in grasses, participating in what has been named as Strategy II for plant iron uptake (in contrast to the Strategy I, used by non-grasses) (Kobayashi & Nishizawa, 2012). Monocots secrete nicotianamine-derived phytosiderophores to the rhizosphere, where they chelate iron and other transition elements (Nozoye et al., 2011; Roberts, Pierson, Panaviene, & Walker, 2004; Schaaf et al., 2004). Subsequently, YSL proteins mediate the uptake of these complexes into root epidermal cells (Curie et al., 2001). However, this is not the only role of YSLs. In both monocots and dicots, YSLs facilitate the transport of metal-nicotianamine complexes as part of a more general role in long-distance metal transport and intracellular transport (DiDonato, Roberts, Sanderson, Easley, & Walker, 2004; Waters et al., 2006). For instance, *Arabidopsis thaliana* YSL1 and YSL3 are responsible for iron uptake from the vascular tissues, redistribution from senescent leaves, and delivery to the seed (Waters et al., 2006). More recently, it has been proposed that YSL proteins also participate in the systemic control of iron homeostasis in plants (Kumar et al., 2017).

Based on their amino acid sequence, YSL transporters can be classified into four different groups (Yordem et al., 2011). Group I includes ZmYS1, AtYSL1 and AtYSL3. Group II is formed by a number of YSL proteins that have intracellular localization. AtYSL4 and AtYSL6 are among the best characterized members of this group. They are located on the tonoplast or in chloroplast membranes, and are involved in the mobilization of metal stores (Conte et al., 2013; Divol et al., 2013). YSL Group IV contains only monocot proteins, and includes metal transporter OsYSL8 (Aoyama et al., 2009). Members from these three groups above have been linked to transition metal

homeostasis (Conte et al., 2013; Curie et al., 2001). In contrast, no physiological function has been attributed to YSLs belonging to Group III.

Group III YSLs, AtYSL7 and AtYSL8 are able to transport peptides into the cell (Hofstetter, Dudnik, Widmer, & Dudler, 2013). Plant pathogen *Pseudomonas syringae* pv *syringae* takes advantage of this ability to introduce the virulence factor SylA, a tripeptide involved in proteasome inhibition that dysregulates the plant immune response, into the plant cell (Groll et al., 2008). It is unlikely that this is the physiological role of Group III YSLs. However, no metal-related phenotype has been reported for *Arabidopsis* mutants in members of this, perhaps as a consequence of the observed functional redundancy within the YSL family (Divol et al., 2013; Waters et al., 2006). As an alternative, we reasoned that the model legume *Medicago truncatula* might be a more appropriate system to study the role of Group III YSLs. This plant has the ability to carry out symbiotic nitrogen fixation, a process that relies on metal transport (González-Guerrero, Escudero, Sáez, & Tejada-Jiménez, 2016). In addition, the establishment of the symbiosis required the neofunctionalization of many genes (De Mita, Streng, Bisseling, & Geurts, 2014), and could have caused the loss of some of the functional redundancy that characterizes the YSL family.

Transition elements are essential for symbiotic nitrogen fixation as cofactors of many of the enzymes participating in this process, including the enzyme central to the conversion of N_2 into NH_4^+ , nitrogenase (Brear, Day, & Smith, 2013; González-Guerrero, Matthiadis, Sáez, & Long, 2014). Many of the genes encoding these metalloenzymes are expressed at high levels, and a substantial fraction of the metals incorporated into the plant is directed to the root nodules, often causing a metal deficiency response (Terry, Soerensen, Jolley, & Brown, 1991). In many cases, dedicated metal transport systems have been adapted from pre-existing ones to ensure proper metal supply to the newly developed organs. When functional redundancy exists in other plant tissues, in the nodule only one of the redundant genes may acquire a new symbiotic role. Here, we take advantage of this possibility to study *M. truncatula* YSL7 (*Medtr3g063490*), a Group III YSL family member with high expression in nodules that is important for plant growth in general and nitrogen fixation in particular.

2 | MATERIALS AND METHODS

2.1 | Plant growth conditions

Medicago truncatula *Tnt1*-insertion mutants *ysl7-1* (NF11536) and *ysl7-2* (NF9504) were identified by PCR-based reverse screening of the *Tnt1* DNA pools as described by Cheng et al. (2014). Seeds from these mutants and from *M. truncatula* R108 (wild type) were scarified, sterilized and germinated as indicated by Tejada-Jiménez et al. (2015). Seedlings were planted in sterile perlite pots and inoculated with *Sinorhizobium meliloti* 2011 or with the same bacterial strain transformed with pHc60-GFP (Cheng & Walker, 1998). Plants were grown

in a greenhouse with the conditions 16 hr light at 25°C and 8 hr dark at 20°C, and watered every 2 days with Jenner's solution alternating with water (Brito, Palacios, Hidalgo, Imperial, & Ruíz-Argüeso, 1994). Nodules were collected at 28 days post-inoculation (dpi). Non-nodulated plants were grown under the same conditions of light and temperature but were watered every 2 weeks with solutions supplemented with 2 mM NH₄NO₃.

Hairy-root transformations of *M. truncatula* seedlings with *Agrobacterium rhizogenes* ARqua1 carrying the appropriate binary vector, were performed following the methodology described by Boisson-Dernier et al. (2001).

2.2 | Yeast complementation assays

To analyse the ability of MtYSL7 to transport peptides, MtYSL7 was amplified using the primers listed in Table S1 and cloned in the *Pst*I and *Xho*I sites of pDR196. Yeast strains $\Delta opt1$ with full disruption of the *YJL212C* (*OPT1*) gene (Euroscarf) (BY4741; *MATa*; *ura3 Δ 0*; *leu2 Δ 0*; *his3 Δ 1*; *met15 Δ 0*; *YJL212c::kanMX4*) and BY4741 (Winston, Dollard, & Ricupero-Hovasse, 1995) were used. Growth experiments were performed using SD medium without nitrogen (N) supplemented with 100 μ M peptides indicated as a nitrogen source. SD medium supplemented with 5 g/L (NH₄)₂SO₄ was used as a growth control media. Tenfold serial dilutions were spotted (5 μ l) onto SD or YPD plates and incubated at 28°C for 2–3 days.

2.3 | Quantitative real-time PCR

Gene expression studies were done using quantitative real-time PCR (RT-qPCR) (StepOne plus, Applied Biosystems) using the Power SyBR Green master mix (Applied Biosystems). Primers used are indicated in Table S1. RNA levels were normalized by using the *ubiquitin carboxy-terminal hydrolase* gene as an internal standard for *M. truncatula* genes (Kakar et al., 2008). RNA isolation and cDNA synthesis were carried out as previously described (Tejada-Jiménez et al., 2015).

2.4 | GUS staining

Two kilobases upstream of the MtYSL7 start codon were amplified using the primers indicated in Table S1, then cloned in pDONR207 (Invitrogen) and transferred to pGWB3 (Nakagawa et al., 2007) using Gateway Cloning technology (Invitrogen). This led to the fusion of the promoter region of MtYSL7 with the *gus* gene in pGWB3. An *A. rhizogenes* ARqua1 derived strain containing pGWB3::MtYSL7_{prom} vector was used for root transformation of *M. truncatula*. Transformed plants were transferred to pots containing sterilized perlite and inoculated with *S. meliloti* 2011. GUS activity was determined in 28 dpi plants as described (Vernoud, Journet, & Barker, 1999).

2.5 | Immunohistochemistry and confocal microscopy

A DNA fragment containing the full length MtYSL7 genomic region and the 2 kb upstream of its start codon was amplified using the primers indicated in Table S1 and cloned into plasmid pGWB13 (Nakagawa et al., 2007) using Gateway technology (Invitrogen). This resulted in the fusion of three C-terminal hemagglutinin (HA) epitopes in-frame. Hairy-root transformation was performed as previously described (Vernoud et al., 1999). Transformed plants were transferred to pots with sterilized perlite and inoculated with *S. meliloti* 2011 containing a pHc60 plasmid derivative that constitutively expresses GFP. Roots and nodules collected from plants 28 dpi were fixed by overnight incubation in 4% paraformaldehyde, 2.5% sucrose in PBS at 4°C. After washing in PBS, nodules were included in 6% agarose and cut in 100 μ m sections with a Vibratome 1,000 plus (Vibratome). Sections were dehydrated using a methanol series (30, 50, 70, 100% in PBS) for 5 min and then rehydrated. Cell walls were permeabilized with 4% cellulase in PBS for 1 hr at room temperature and with 0.1% Tween 20 in PBS for 15 min. Sections were blocked with 5% bovine serum albumin (BSA) in PBS before their incubation with an anti-HA mouse monoclonal antibody (Sigma) for 2 hr at room temperature. After washing, an Alexa594-conjugated anti-mouse rabbit monoclonal antibody (Sigma) was added to the sections for 1 hr at room temperature. DNA was stained with DAPI after washing. Images were acquired with a confocal laser-scanning microscope (Leica SP8) using excitation lights at 488 nm for GFP and at 561 nm for Alexa 594.

2.6 | Acetylene reduction assay

Nitrogenase activity was measured by the acetylene reduction assay (Hardy, Holsten, Jackson, & Burns, 1968). Nitrogen fixation was assayed in mutants and control plants at 28 dpi in 30 ml vials fitted with rubber stoppers. Each vial contained four to five pooled transformed plants. Three milliliter of air inside the vial were replaced with 3 ml of acetylene to start the reaction, and vials were incubated at room temperature for 30 min. Gas samples (0.5 ml) were analysed in a Shimadzu GC-8A gas chromatograph fitted with a Porapak N column. The amount of ethylene produced was determined by measuring the height of the ethylene peak relative to the background. Each data point was estimated from two different vials. After measurements, nodules were recovered from roots to measure their weight.

2.7 | Metal content determination

Iron content was determined in shoots, roots and nodules 28 dpi using Atomic Absorption Spectroscopy (AAS) or Inductively Coupled Plasma-Mass Spectrometry (ICP-MS). Plant tissues for AAS were weighted and mineralized in 15.6 M HNO₃ (trace metal grade) for 1 hr

at 80°C and overnight at 20°C. Digestions were completed with 2 M H₂O₂. Samples were diluted in 300 mM HNO₃ before measurements. Element analyses were performed in an AAnalyst 800 (Perkin Elmer), equipped with a graphite furnace. All samples were measured in duplicate. ICP-MS analyses were carried out at the Unit of Metal Analysis in the Scientific and Technology Centre of Universidad de Barcelona (Spain).

2.8 | Bioinformatics

To identify *M. truncatula* YSL family members, BLASTN and BLASTX searches were carried out in the *M. truncatula* Genome Project site (<http://www.jcvi.org/medicago/index.php>). Protein sequences for tree construction were obtained from Phytozome (<https://phytozome.jgi.doe.gov/pz/portal.html>), Uniprot (<http://www.uniprot.org/blast>) and NCBI (<https://blast.ncbi.nlm.nih.gov/Blast.cgi?PAGE=Proteins>) as follows: *M. truncatula* MtYSL1 (Medtr1g077840); MtYSL2 (Medtr1g007540); MtYSL3 (Medtr3g092090); MtYSL4 (Medtr1g007580); MtYSL5 (Medtr6g077870); MtYSL6 (Medtr7g028250); MtYSL7 (Medtr3g063490), MtYSL8 (Medtr5g091600) and MtYSL9 (Medtr3g063520); *Arabidopsis thaliana* AtYSL1 (At4g24120), AtYSL2 (At5g24380), AtYSL3 (At5g53550), AtYSL4 (At5g41000), AtYSL5 (At3g17650), AtYSL6 (At3g27020), AtYSL7 (At1g65730), AtYSL8 (At1g48370); *Oryza sativa* OsYSL1 (Os01g0238700), OsYSL3 (Os05g0251900), OsYSL4 (Os05g0252000); OsYSL5 (Os04g0390600), OsYSL6 (Os04g0390500); OsYSL7 (Os02g0116300), OsYSL8 (Os02g0116400), OsYSL10 (Os04g0674600), OsYSL12 (Os04g0524600), OsYSL13 (Os04g0524500), OsYSL14 (Os02g0633300); OsYSL15 (Os02g0650300), OsYSL16 (Os04g0542800); OsYSL17 (Os08g0280300), OsYSL18 (Os01g0829900); *Zea mays* ZmYSL1 (Zm00001d017429), ZmYSL2 (Zm00001d025977), ZmYSL6 (Zm00001d003941), ZmYSL11 (Zm00001d025888), ZmYSL12 (Zm00001d025887), ZmYSL14A (Zm00001d051193), ZmYSL17 (Zm00001d054042); *Brachypodium distachyon* BdYSL1A (BRADI_3g50267), BdYSL1B (BRADI_3g50263), BdYSL2 (BRADI_3g50260), BdYSL3 (BRADI_5g17230), BdYSL9 (BRADI_5g17210); BdYSL10 (BRADI_2g5395), BdYSL11 (BRADI_5g16190), BdYSL12 (BRADI_5g16170), BdYSL13 (BRADI_5g16160) and *Glycine max* GmYSL7 (GLYMA_11G203400), GLYMA_09G164500; GLYMA_16G212900.

Trees were constructed from a ClustalW multiple alignment of the sequences (<http://www.ebi.ac.uk/Tools/msa/clustalw2>), then analysed with MEGA7 (S. Kumar, Stecher, & Tamura, 2016) using a Neighbour-Joining algorithm with bootstrapping (1,000 iterations). Unrooted trees were visualized with FigTree (<http://tree.bio.ed.ac.uk/software/figtree>).

2.9 | Statistical tests

Data were analysed with Mann–Whitney test to calculate the statistical significance of observed differences. Test results with *p* values lower than .05 were considered as statistically significant.

3 | RESULTS

3.1 | MtYSL7 is expressed in roots and in nodules

The *M. truncatula* genome contains nine YSL genes (*MtYSL1*–*MtYSL9*). Sequence comparison of the encoded proteins with known YSL proteins from monocots and dicots, showed that *M. truncatula* YSLs are distributed in the same groups as any other dicot (Figure 1a). Four of them (*MtYSL1*–4) belonged to Group I, one (*MtYSL6*) is clustered in group II and four (*MtYSL5*, 7, 8 and 9) were in Group III. *MtYSL7* was very similar to *AtYSL7* and *GmYSL7*, and likely resulted from a duplication event with *MtYSL8* or *MtYSL9*. *MtYSL7*, *MtYSL8* and *MtYSL9* were over 89% identical.

MtYSL7 was the only gene among the four members of the Group III *M. truncatula* YSLs to have a maximum expression in nodules (Figures 1b and S1). Transcripts of this gene were specifically detected in roots and nodules, with no significant transcription in shoots. In spite of their high degree of similarity to *MtYSL7*, *MtYSL8* and *MtYSL9* were not expressed in nodules. In fact, no *MtYSL8* or *MtYSL9* transcripts were found in any organs at the time points analysed (Figure S1). In contrast, *MtYSL5* was expressed in all organs tested, with the lowest relative expression detected in nodules.

3.2 | MtYSL7 is a peptide transporter

YSL transporters have been typically associated with the transport of transition metal complexed with non-proteogenic amino acid nicotianamine or its derivatives (Schaaf et al., 2004). To test whether *MtYSL7* was able to transport transition elements either free or complexed with nicotianamine, complementation assays of *S. cerevisiae* metal transport mutants were carried out. For this, the strains *ctr1* (deficient in copper uptake), *zrt1zrt2* (deficient in zinc uptake) and *fet3fet4* (deficient in iron uptake) were used (Askwith et al., 1994; Dancis et al., 1994; Dix, Bridgham, Broderius, Byersdorfer, & Eide, 1994; Zhao & Eide, 1996). These strains were co-transformed with a plasmid expressing a β -estradiol-dependent transactivator of *Gal* promoters, and a plasmid containing the *MtYSL7* coding sequence regulated by a *Gal* promoter. Drop tests were carried out using serial dilutions of the cultures. In the case of iron, both Fe²⁺ and Fe³⁺ forms were tested. As shown in Figure S2, there was no restoration of the wild-type growth for any of the conditions tested, unlike what has been reported for other metal-nicotianamine transporting YSLs in similar assays (Waters et al., 2006).

Another possibility is that the substrate of *MtYSL7* is a peptide and not a metal-NA complex, given that YSL and OPT proteins are closely related (Lubkowitz, 2011), and that *Arabidopsis* *AtYSL7* transports a peptide (Hofstetter et al., 2013). To test this possibility, different peptides were provided as the sole nitrogen source to an *S. cerevisiae* strain lacking an oligopeptide transporter (*opt1*) (Osawa, Stacey, & Gassmann, 2006) and transformed with a plasmid containing *MtYSL7* (Figure 2). *MtYSL7*-expressing yeasts were able to grow when four to six amino acid peptides were provided. Some limited growth was also observed when a 12 amino acid peptide was used as a substrate, but not when one of 10 was provided. *MtYSL7*

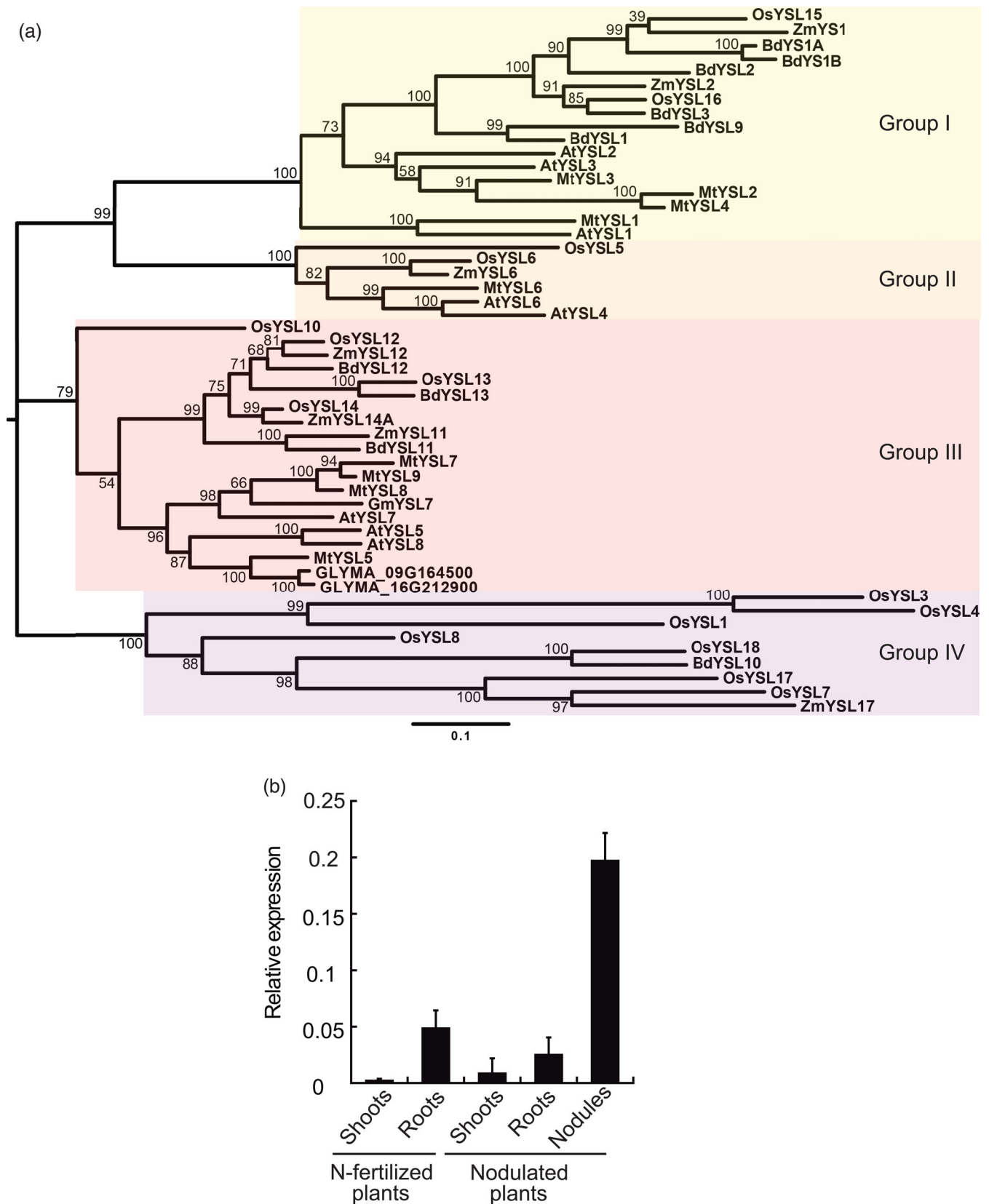


FIGURE 1 *Medicago truncatula* YSL7 is a Group III YSL highly expressed in nodules. (a) Unrooted tree of the *M. truncatula* YSL transporters, MtYSL1-MtYSL9 (Medtr1g077840, Medtr1g007540, Medtr3g092090, Medtr1g007580, Medtr6g077870, Medtr7g028250, Medtr3g063490, Medtr5g01600, and Medtr3g063520, respectively), and representative plant homologues. Numbers indicate bootstrapping values. (b) *MtYSL7* expression relative to internal standard gene *ubiquitin carboxyl-terminal hydrolase*. Data are the $M \pm SE$ of five independent experiments

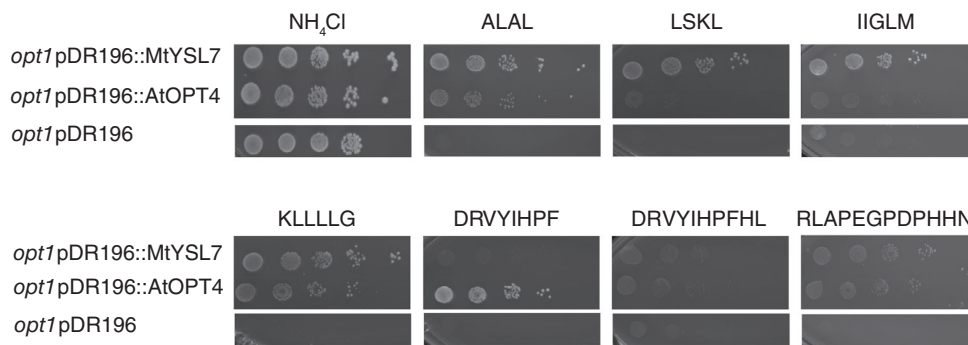
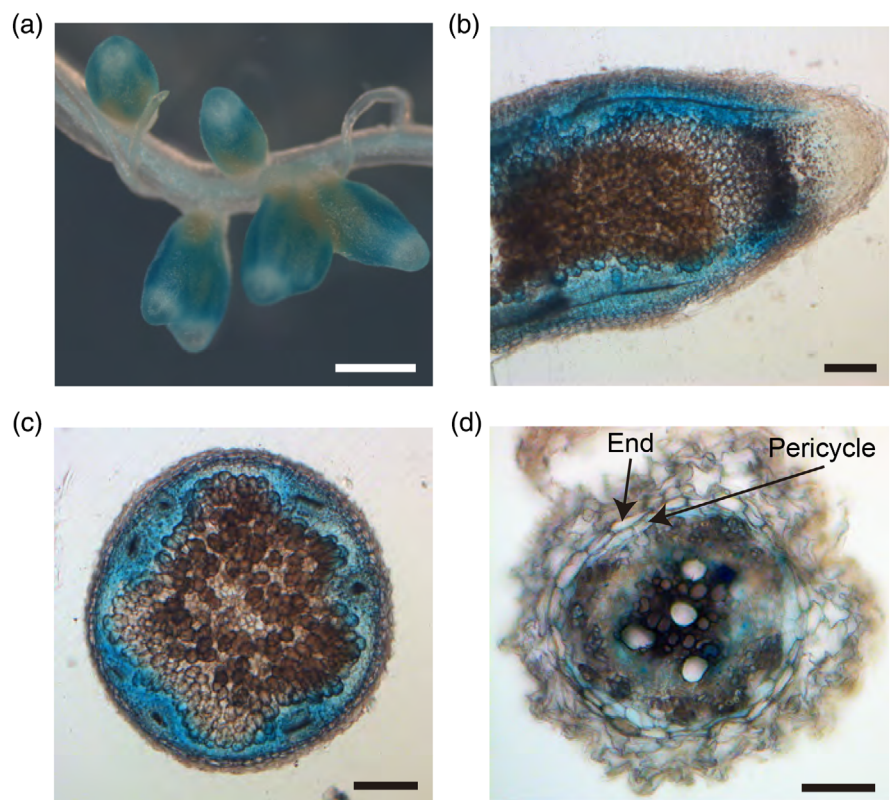


FIGURE 2 MtYSL7 transports peptides. The yeast strain *opt1*, mutant in the oligopeptide transporter ScOPT1, was transformed with either the empty pDR196 vector, or with pDR196 containing the coding sequence of MtYSL7 or AtOPT4. Serial dilutions (10x) were grown on SD media supplemented with the nitrogen sources indicated. The selected are representative images from at least three independently carried experiments using each a different yeast transformant

FIGURE 3 MtYSL7 is expressed in the root and nodule vasculature and in the nodule cortex. Histochemical staining of the GUS activity in 28 dpi root and nodules expressing the *gus* gene under the regulation of the MtYSL7 promoter. (a) General view of both root and nodule. Bar = 1 mm. (b) Longitudinal section of a nodule. Bar = 200 μ m. (c) Cross section of nodule. Bar = 200 μ m. (d) Cross section of a root. Bar = 100 μ m. The images shown are representative images from four separate *M. truncatula* transformations, each producing at least 15 plants, whose roots and nodules were collected and prepared for GUS expression determination [Colour figure can be viewed at wileyonlinelibrary.com]



did not appear to transport the tripeptide glutathione when expressed in the yeast glutathione transport mutant *hgt* (Figure S3). In addition, no evidence for the transport of iron-regulatory peptide IMA (Grillet, Lan, Li, Mokkapat, & Schmidt, 2018) was observed (Figure S4).

3.3 | MtYSL7 is located in the plasma membrane of root pericycle and nodule cortical cells

To determine the tissue localization of MtYSL7 expression, *M. truncatula* seedlings were transformed with a construct fusing the

2 kb region upstream of MtYSL7 to the β -glucuronidase gene (*gus*). GUS activity was localized in plants 28 dpi based on the blue stain resulting from using X-Gluc as a substrate (Figure 3). In agreement with the RT-qPCR studies (Figure 1b), MtYSL7 was expressed in roots and nodules, with a more intense signal in nodules (Figure 3a). In nodules, MtYSL7 expression was located in the cortical region of the nodule throughout its length (Figure 3b,c), and no expression was observed in the nodule core, regardless of the developmental zone of the nodule. In roots, GUS activity was detected in the perivascular region, in a zone that contains the pericycle surrounding the vessels (Figure 3d).

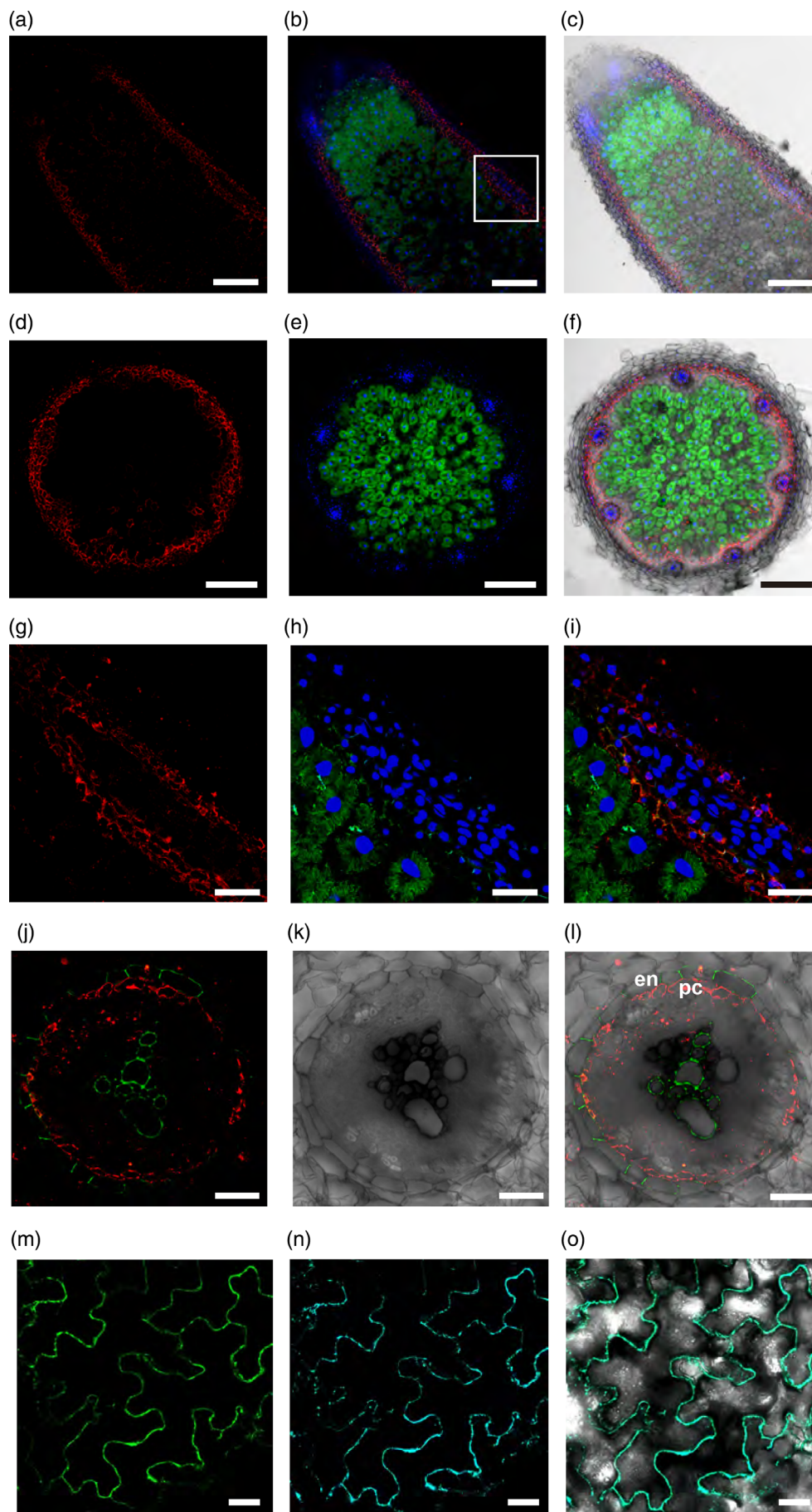


FIGURE 4 Legend on next page.

A C-terminal (HA)₃-tagged MtYSL7 was expressed from a construct regulated by its own promoter and the localization detected using an anti-HA Alexa 594-conjugated antibody. The results of the immunolocalization supported the above reporter gene studies (Figure 4). The fluorescent signal from the Alexa 594-conjugated antibody used to localize MtYSL7-HA was observed in the periphery of the nodule, in the cortical area, both in the perivascular and intervascular areas (Figure 4a–f). At a higher magnification, MtYSL7-HA appeared to be confined to the endodermal layer (Figures 4g–i and S5), and mostly to the periphery of the cell. In roots, MtYSL7-HA was observed in the pericycle (Figure 4j–l). The intracellular distribution of MtYSL7-HA was indicative of a plasma membrane association, and this was supported by its co-localization with a plasma membrane marker when co-transfected into tobacco leaves (Figure 4m–o). Controls in the absence of Alexa 594-conjugated antibody did not show any signal in the measured channels (Figure S6). Finally, these antibodies did not exhibit any binding capabilities in nodules not expressing an HA-tagged protein (Castro-Rodríguez et al., 2020).

3.4 | MtYSL7 mutation affects plant growth and symbiotic nitrogen fixation

To determine the function of MtYSL7, two *M. truncatula* *Tnt1* insertional mutants were obtained from the Noble Research Institute (Tadege et al., 2008). NF11536 (*ysl7-1*) is a knock-down line with the transposon inserted in its first intron (nucleotide +1,118) (Figure 5a). The *Tnt1* insertion in NF9504 (*ysl7-2*) is in the first exon at nucleotide +315, and reduces MtYSL7 expression below our detection limit. Both MtYSL7 mutant alleles exhibited reduced growth compared to wild type plants when grown with ammonium nitrate in the medium (Figure 5b,c). The growth phenotype, particularly in roots, was restored in the knock-out *ysl7-2* mutant allele when a wild-type copy of MtYSL7-HA expressed under the

control of its own promoter was reintroduced (Figure S7). In addition, although it was not evident from visual examination of the plants, both mutant alleles had a slight but significant reduction in chlorophyll content (Figure 5d). In general, no significant differences in iron, copper or zinc concentrations were observed, the one exception being copper levels in shoots of *ysl7-2* (Figure 5e–g).

Similar growth differences were observed when the symbiosis with *S. meliloti* was the only source of nitrogen (Figure 6). Plant growth was reduced in MtYSL7 mutants, to a higher degree in the knock-out line than the knock-down line (Figure 6a,b). These plants developed nodules that were morphologically similar to wild-type nodules (Figure 6c), but their nitrogenase activity was reduced by ca. 60% in both *Tnt1* lines (Figure 6d). These phenotypes were restored in *ysl7-2* when a wild-type copy of MtYSL7-HA expressed under its native promoter was reintroduced (Figure S8). In addition, the iron and copper content of *ysl7-2* nodules was significantly higher than in those of wild type (Figure 6e,f), while no differences were observed for zinc (Figure 6g). Increased iron concentrations might be the result of the increased expression in roots of iron uptake and delivery systems, such as ferredoxinase FRO1 and iron transporter MtNRAMP1 (Figure 7). The genes encoding these proteins were expressed at higher levels in roots of both *ysl7-1* and *ysl7-2* plants grown in symbiotic conditions, although the induction was much higher in *ysl7-2* roots. The expression levels of these genes were not affected under non-symbiotic conditions (Figure S9). The increased iron content in *ysl7-2* nodules did not result in the altered iron distribution in nodules (Figure S10). Knock-down *ysl7-1* showed a similar, although not statistically significant pattern of metal accumulation (Figure 6e–g), probably as a consequence of the remaining MtYSL7 expression (Figure 5c). In spite of the altered iron and copper homeostasis in nodules, reducing or increasing iron or copper content in the nutrient solution did not have any significant effect on plant growth or nitrogenase activity (Figures S11 and S12).

FIGURE 4 MtYSL7 is located in the periphery of nodule cortical cells, in the nodule endodermis and in the root pericycle. (a–c) Longitudinal section of a 28 dpi *M. truncatula* nodule expressing MtYSL7 under its own promoter and fused to three HA epitopes (MtYSL7-HA). The HA-tag was detected with the help of a secondary Alexa594-conjugated antibody (red, a). Transformed plants were inoculated with a GFP-expressing *S. meliloti* (green) and DNA was stained with DAPI (blue, b). C shows the overlay of all these channels together with the bright field image. Bars = 200 µm. (d–f) Cross section of a 28 dpi *M. truncatula* nodule expressing MtYSL7-HA and detected with an Alexa594-conjugated antibody (red, d). Transformed plants were inoculated with a GFP-expressing *S. meliloti* (green) and DNA was stained with DAPI (blue, e). Panel F shows the overlay of all these channels together with the bright field image. Bars = 200 µm. (g–i) Detail of a longitudinal section of a vessel from a 28 dpi *M. truncatula* nodule expressing MtYSL7-HA and detected with an Alexa594-conjugated antibody (red, g) and inoculated with GFP-expressing *S. meliloti* (green). DNA was stained with DAPI (blue, h). Panel I shows the overlay of all these channels. The arrowheads indicate the position of the Casparian strip. Bars = 50 µm. (j–l) Cross section of a 28 dpi root expressing MtYSL7-HA and detected with an Alexa594-conjugated antibody (red). Lignin autofluorescence was used to identify xylem and Casparian strip lignin (green, j). Panel K shows the brightfield image and all three channels are overlaid in panel L. Endodermis (en) and pericycle (pc) are indicated. Bars = 50 µm. (m–o) Colocalization of MtYSL7-GFP and AtPIP2-CFP in tobacco leaves. Left panel shows the localization of MtYSL7 fused to GFP (green, m) transiently expressed in tobacco leaf cells. Middle panel shows the localization of plasma membrane marker AtPIP2 fused to CFP (cyan, n), transiently expressed in the same cells. Panel O is the overlay of the two previous channels together with the bright field image. Bars = 50 µm. The images shown are representative images from four separate *M. truncatula* transformations, each producing at least 15 plants, whose roots and nodule were collected and prepared for GUS expression determination [Colour figure can be viewed at wileyonlinelibrary.com]

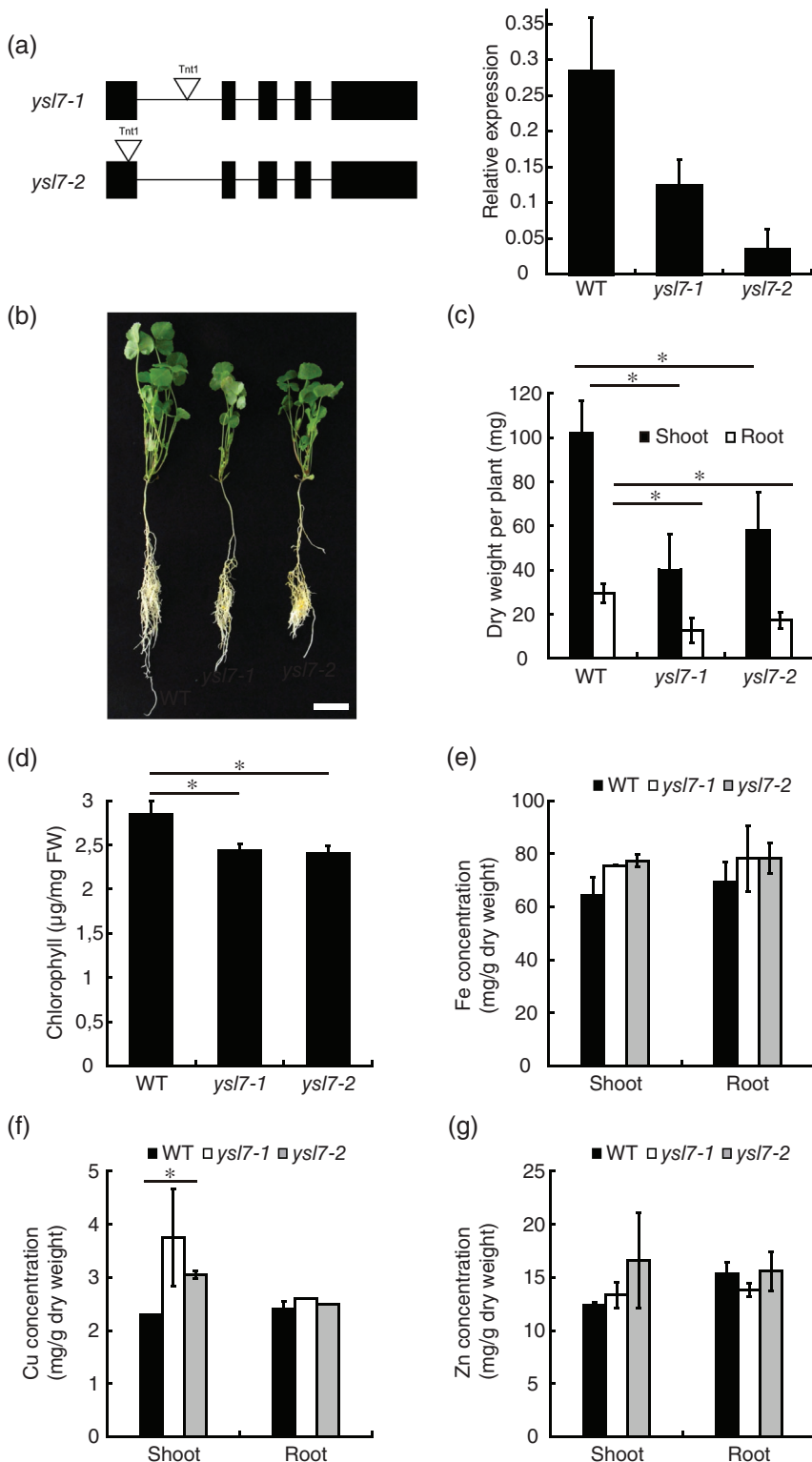


FIGURE 5 *MtYSL7* mutation affects plant growth under non-symbiotic conditions.

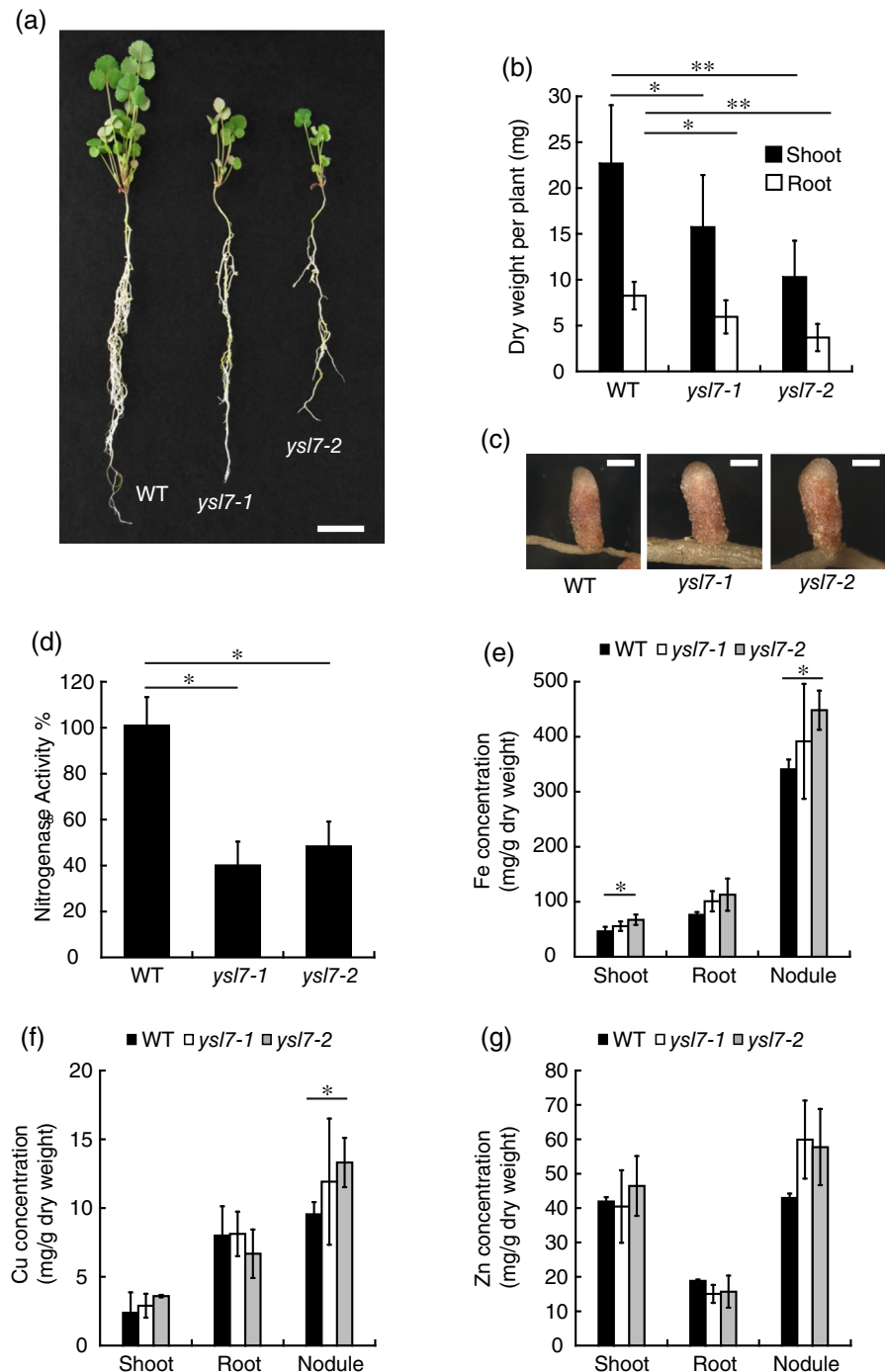
(a) Position of the *Tnt1* insertions in *ysl7-1* and *ysl7-2* lines (left side). Right side, *MtYSL7* expression in 28 dpi nodules from WT, *ysl7-1*, and *ysl7-2* plants relative to internal standard gene *ubiquitin carboxyl-terminal hydrolase*. Data are the $M \pm SE$ of three independent experiments. (b) Growth of representative plants. Bar = 3 cm. (c) Dry weight of shoots and roots of wild type, *ysl7-1* and *ysl7-2* plants. Data are the $M \pm SE$ ($n = 5$ plants). (d) Chlorophyll content of wild type, *ysl7-1* and *ysl7-2* shoots. Data are the $M \pm SE$ of three sets of five pooled plants. (e) Iron content in roots and shoots of wild type, *ysl7-1* and *ysl7-2* plants. Data are the $M \pm SE$ of five sets of five pooled plants. (f) Copper content in roots and shoots of wild type, *ysl7-1*, and *ysl7-2* plants. Data are the $M \pm SE$ of five sets of five pooled plants. (g) Zinc content in roots and shoots of wild type, *ysl7-1* and *ysl7-2* plants. Data are the $M \pm SE$ of five sets of five pooled plants. Asterisk indicates statistical significance ($p < .05$) [Colour figure can be viewed at wileyonlinelibrary.com]

4 | DISCUSSION

YSLs play a role in transition metal uptake from the soil, its distribution from source to sink tissues, as well as in intracellular metal remobilization (Conte et al., 2013; Curie et al., 2001; Waters et al., 2006). More recently, YSL proteins have been implicated in long-distance signalling of the nutritional status of iron (Kumar

et al., 2017). These functions are carried out by members of three of the four known YSL groups (Yordem et al., 2011). The remaining one, Group III, has been associated with the transport of the *P. syringae* pv. *syringae* virulence factor *SylA* (Hofstetter et al., 2013). Although it is unlikely that this is its physiological role, it showcases the ability of proteins from this family to use peptides as their substrate. We were able to show that *MtYSL7* can act as a peptide transporter, since its

FIGURE 6 MtYSL7 participates in symbiotic nitrogen fixation. (a) Growth of representative wild type, *ysl7-1* and *ysl7-2* plants. Bar = 3 cm. (b) Dry weight of shoots and roots of 28 dpi plants. Data are the $M \pm SE$ ($n = 10-15$ plants). (c) Detail of representative nodules of 28 dpi wild type, *ysl7-1* and *ysl7-2* plants. Bars = 1 mm. (d) Nitrogenase activity in 28 dpi nodules from wild type, *ysl7-1* and *ysl7-2* plants. Data are the $M \pm SE$ measured in duplicate from three sets of five pooled plants. 100% = 0.28 nmol ethylene/hr/plant. (e) Iron content in roots, shoots, and nodules of wild type, *ysl7-1* and *ysl7-2* plants. Data are the $M \pm SE$ of five sets of five pooled plants. (f) Copper content in roots, shoots and nodules of wild type, *ysl7-1* and *ysl7-2* plants. Data are the $M \pm SE$ of five sets of five pooled plants. (g) Zinc content in roots, shoots and nodules of wild type, *ysl7-1* and *ysl7-2* plants. Data are the $M \pm SE$ of five sets of five pooled plants. Asterisk indicates statistical significance ($p < .05$) [Colour figure can be viewed at wileyonlinelibrary.com]



expression restored the uptake capacity for short peptides in yeast. However, there appeared to be some specificity in MtYSL7-mediated transport, since a decapeptide was not transported, and neither were the tripeptide glutathione or IMA-related peptides consisting of four, five or seventeen amino acids.

MtYSL7 was expressed in roots and nodules, with the highest levels observed in the nodules. Immunolocalization of HA-tagged MtYSL7 indicated that it is associated with the plasma membrane of cells in the root pericycle and in the nodule cortex and vasculature, a subcellular localization similar to that of AtYSL7 (Hofstetter

et al., 2013). In roots, it could be hypothesized that MtYSL7 could be introducing a yet-to-be determined metal complex into the pericycle cell, either from the root cortex or from the root vessels. In this situation, *ysl7* mutant roots should have altered metal levels, but they do not. In addition, this hypothetical role of MtYSL7 as a metal-complex transporter would mean that in the nodule cortex cells, MtYSL7 would be introducing metals, possibly iron in view of the metal content of the *ysl7-2* mutant, into a cell layer with a specific need for them, with a role in preventing oxygen diffusion into the nodule. This would create an iron pool separated from that directed for nitrogen-fixing cells,

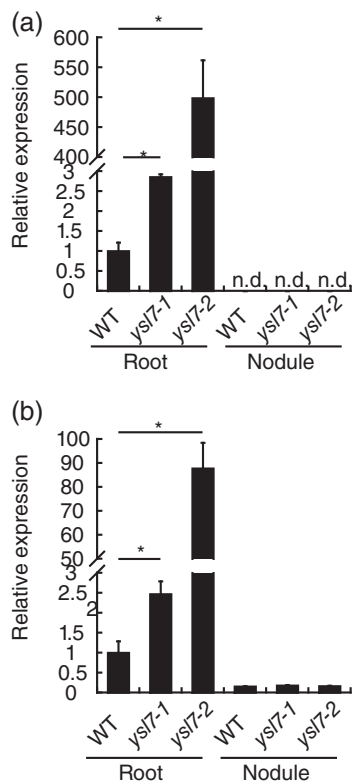


FIGURE 7 Mutation of *MtYSL7* alters the expression of iron homeostasis genes in nodulated plants. (a) *MtFRO1* expression relative to internal standard gene *ubiquitin carboxyl-terminal hydrolase* in 28 dpi roots and nodules from wild type (WT), *ysl7-1* and *ysl7-2* plants. Data bars are standardized to wild type values (1) and show the $M \pm SE$ of three independent experiments. (b) *MtNRAMP1* expression relative to internal standard gene *ubiquitin carboxyl-terminal hydrolase* in 28 dpi roots and nodules from wild type (WT) *ysl7-1* and *ysl7-2* plants. Data bars are standardized to wild type values (1) and show the $M \pm SE$ of three independent experiments. Asterisk indicates statistical significance ($p < .05$)

which very likely is in the form of iron-citrate (Kryvoruchko et al., 2018; Tejada-Jiménez et al., 2015). It would also explain the reduction of nitrogenase activity observed, a result of some oxygen leaking to the interior of the nodule, poisoning nitrogenase. However, if this were the case, we should expect that metal fortification of the nutrient solution would partially complement the phenotype, as reported for other nodule metal transport mutants (Gil-Díez et al., 2019; Tejada-Jiménez et al., 2015, 2017). Moreover, we should also observe metal accumulation in the apoplast around these cells. The fact that this did not happen could be explained either because of the absence of an additional low affinity metal uptake system in those cells or because *MtYSL7* is playing a different physiological function.

An alternative hypothesis for the role of *MtYSL7* is that its substrate transmits a peptide signal somehow linked to metal homeostasis. Blocking the transport capabilities of the signal would alter metal-dependent processes, among others, and could explain the small reduction of chlorophyll content observed and the altered plant growth. In nodules, sensing low-iron levels would lead to reduced

nitrogenase assembly, which would also explain the reduced activity observed. Supporting this theory is the observed increase in iron and copper content of *ysl7-2* nodules, perhaps the consequence of the lack of a feedback signal to indicate metal sufficiency in nodules. Since no change in iron distribution was observed, it could be speculated that no defects in overall metal transport would result from loss of *MtYSL7* function. In addition, consistent with this hypothesis is the upregulation of iron uptake systems in roots of nodulated *ysl7* mutants. *MtFRO1* is a ferredoxinase involved in the iron deficiency response in roots, responsible for the conversion of Fe^{3+} to Fe^{2+} prior to its assimilation (Andaluz, Rodríguez-Celma, Abadía, Abadía, & López-Millán, 2009). Upregulation of *MtFRO1* in roots would usually be the result of iron deficiency in the plant. However, in *ysl7* mutants there was no significant reduction of iron concentration in the plant; there were higher iron concentrations in *ysl7-2* nodules instead. Similarly, *MtNramp1* expression levels were higher in the roots of *ysl7-2* plants than in the controls, while no statistical differences were observed in nodules. *MtNramp1* is responsible for iron uptake by the root endodermis and by rhizobia-infected nodule cells (Tejada-Jiménez et al., 2015). The fact that it is upregulated exclusively in roots may indicate that a signal controlling whole plant metal iron allocation has been disrupted rather than one related only to nitrogen-fixing cells. Similarly, *GmYSL7*, a close orthologue of *MtYSL7* in soybean, can functionally complement the *ysl7* phenotype when driven under the *MtYSL7* promoter (Gavrin et al., 2021). *GmYSL7* is a nodule-specific protein, located on the symbiosome membrane, with similar peptide transport characteristics, that might synchronize the metabolism/nutrition between the macro- and microsymbionts, including metal homeostasis genes. This different subcellular localization in the two legumes may reflect the different requirements for controlling nodule functioning in indeterminate and determinate type nodules.

Regardless of the specific cause for the induction of Fe deficiency responses in the root in the *ysl7* mutants, these results link Group III YSL function to metal homeostasis, a physiological role shared by all the other three YSL groups (Aoyama et al., 2009; Conte et al., 2013; Curie et al., 2001). This role has been suggested by other studies, but had not been previously demonstrated. To conclusively prove any of these alternative theories presented here, future work should focus on the identification of the specific substrate of Group III YSLs, work which may identify a new group of peptide signals.

ACKNOWLEDGMENTS

This research was funded by a Ministerio de Economía y Competitividad grant (AGL2015-65866-P), a European Research Council Starting Grant (ERC-2013-StG-335284) to M.G.G. and Australian Research Council Industrial Transformation Research Hub (IH140100013). R.C.-R. was supported by a Formación del Personal Investigador Fellowship (BES-2013-062674). V.E. was partially funded by the Severo Ochoa Programme for Centres of Excellence in R&D from Agencia Estatal de Investigación of Spain (grant SEV-2016-0672) to C.B.G.P. Development of *M. truncatula Tnt1* mutant population was, in part, funded by the National Science Foundation,

USA (DBI-0703285) to K.S.M. We acknowledge the other members of laboratory 281 at Centro de Biotecnología y Genómica de Plantas (UPM-INIA) for their support and feedback in preparing this manuscript.

CONFLICT OF INTEREST

The authors declare that they have no conflict of interest.

DATA AVAILABILITY STATEMENT

The data that support the findings of this study are available from the corresponding author upon reasonable request.

ORCID

María Reguera  <https://orcid.org/0000-0001-5939-8576>

Julia Quintana  <https://orcid.org/0000-0002-5145-3590>

Kirankumar S. Mysore  <https://orcid.org/0000-0002-9805-5741>

Penelope M. C. Smith  <https://orcid.org/0000-0001-9841-1112>

Manuel González-Guerrero  <https://orcid.org/0000-0001-7334-5286>

REFERENCES

- Andaluz, S., Rodríguez-Celma, J., Abadía, A., Abadía, J., & López-Millán, A. F. (2009). Time course induction of several key enzymes in *Medicago truncatula* roots in response to Fe deficiency. *Plant Physiology and Biochemistry*, 47, 1082–1088.
- Aoyama, T., Kobayashi, T., Takahashi, M., Nagasaka, S., Usuda, K., Kakei, Y., ... Nishizawa, N. K. (2009). OsYSL18 is a rice iron(III)-deoxymugineic acid transporter specifically expressed in reproductive organs and phloem of lamina joints. *Plant Molecular Biology*, 70, 681–692.
- Askwith, C., Eide, D., Van, H. A., Bernard, P. S., Li, L., Davis-Kaplan, S., ... Kaplan, J. (1994). The *FET3* gene of *S. cerevisiae* encodes a multicopper oxidase required for ferrous iron uptake. *Cell*, 76, 403–410.
- Beadle, G. W. (1929). Yellow stripe—a factor for chlorophyll deficiency in maize located in the Pr pr chromosome. *The American Naturalist*, 63, 189–192.
- Boisson-Dernier, A., Chabaud, M., Garcia, F., Bécard, G., Rosenberg, C., & Barker, D. G. (2001). *Agrobacterium rhizogenes*-transformed roots of *Medicago truncatula* for the study of nitrogen-fixing and endomycorrhizal symbiotic associations. *Molecular Plant-Microbe Interactions*, 14, 695–700.
- Brear, E. M., Day, D. A., & Smith, P. M. C. (2013). Iron: An essential micro-nutrient for the legume–rhizobium symbiosis. *Frontiers in Plant Science*, 4, 359.
- Brito, B., Palacios, J. M., Hidalgo, E., Imperial, J., & Ruiz-Argüeso, T. (1994). Nickel availability to pea (*Pisum sativum* L.) plants limits hydrogenase activity of *Rhizobium leguminosarum* bv. *viciae* bacteroids by affecting the processing of the hydrogenase structural subunits. *Journal of Bacteriology*, 176, 5297–5303.
- Castro-Rodríguez, R., Abreu, I., Reguera, M., Novoa-Aponte, L., Mijovilovich, A., Escudero, V., ... González-Guerrero, M. (2020). The *Medicago truncatula* Yellow Stripe1-Like3 gene is involved in vascular delivery of transition metals in root nodules. *Journal of Experimental Botany*, 71, 7257–7269.
- Cheng, H. P., & Walker, G. C. (1998). Succinoglycan is required for initiation and elongation of infection threads during nodulation of alfalfa by *Rhizobium meliloti*. *Journal of Bacteriology*, 180, 5183–5191.
- Cheng, X., Wang, M., Lee, H. K., Tadege, M., Ratet, P., Udvardi, M., ... Wen, J. (2014). An efficient reverse genetics platform in the model legume *Medicago truncatula*. *New Phytologist*, 201, 1065–1076.
- Conte, S. S., Chu, H. H., Rodríguez, D. C., Punshon, T., Vasques, K. A., Salt, D. E., & Walker, E. L. (2013). *Arabidopsis thaliana* yellow Stripe1-Like4 and yellow Stripe1-Like6 localize to internal cellular membranes and are involved in metal ion homeostasis. *Frontiers in Plant Science*, 4, 283.
- Curie, C., Cassin, G., Couch, D., Divol, F., Higuchi, K., Le Jean, M., ... Mari, S. (2008). Metal movement within the plant: Contribution of nicotianamine and yellow stripe 1-like transporters. *Annals of Botany*, 103, 1–11.
- Curie, C., Panaviene, Z., Loulergue, C., Dellaporta, S. L., Briat, J.-F., & Walker, E. L. (2001). Maize yellow stripe1 encodes a membrane protein directly involved in Fe(III) uptake. *Nature*, 409, 346–349.
- Dancis, A., Yuan, D. S., Haile, D., Askwith, C., Eide, D., Moehle, C., ... Klausner, R. D. (1994). Molecular characterization of a copper transport protein in *S. cerevisiae*: An unexpected role for copper in iron transport. *Cell*, 76, 393–402.
- De Mita, S., Streng, A., Bisseling, T., & Geurts, R. (2014). Evolution of a symbiotic receptor through gene duplications in the legume–rhizobium mutualism. *New Phytologist*, 201, 961–972.
- DiDonato, R. J., Roberts, L. A., Sanderson, T., Eisley, R. B., & Walker, E. L. (2004). *Arabidopsis* Yellow Stripe-Like2 (YSL2) a metal-regulated gene encoding a plasma membrane transporter of nicotianamine-metal complexes. *Plant Journal*, 39, 403–414.
- Divol, F., Couch, D., Conéjéro, G., Roschttardt, H., Mari, S., & Curie, C. (2013). The *Arabidopsis* YELLOW STRIPE LIKE4 and 6 transporters control iron release from the chloroplast. *Plant Cell*, 25, 1040–1055.
- Dix, D. R., Bridgman, J. T., Broderius, M. A., Byersdorfer, C. A., & Eide, D. J. (1994). The *FET4* gene encodes the low affinity Fe(II) transport protein of *Saccharomyces cerevisiae*. *Journal of Biological Chemistry*, 269, 26092–26099.
- Gavrin, A., Loughlin, P. C., Brear, E. M., Griffith, O. W., Bedon, F., Suter, G. M., ... Smith, P. M. C. (2021). Soybean yellow stripe-like7 is a symbiosome membrane peptide transporter essential for nitrogen fixation. *Plant Physiology*. <https://doi.org/10.1093/plphys/kiab044/6129112>
- Gil-Díez, P., Tejada-Jiménez, M., León-Mediavilla, J., Wen, J., Mysore, K. S., Imperial, J., & González-Guerrero, M. (2019). MtMOT1.2 is responsible for molybdate supply to *Medicago truncatula* nodules. *Plant Cell & Environment*, 42, 310–320.
- González-Guerrero, M., Escudero, V., Sáez, Á., & Tejada-Jiménez, M. (2016). Transition metal transport in plants and associated endosymbionts. Arbuscular mycorrhizal fungi and rhizobia. *Frontiers in Plant Science*, 7, 1088.
- González-Guerrero, M., Matthiadis, A., Sáez, Á., & Long, T. A. (2014). Fixating on metals: New insights into the role of metals in nodulation and symbiotic nitrogen fixation. *Frontiers in Plant Science*, 5, 45.
- Grillet, L., Lan, P., Li, W., Mokkaipati, G., & Schmidt, W. (2018). IRON MAN is a ubiquitous family of peptides that control iron transport in plants. *Nature Plants*, 4, 953–963.
- Groll, M., Schellenberg, B., Bachmann, A. S., Archer, C. R., Huber, R., Powell, T. K., ... Dudler, R. (2008). A plant pathogen virulence factor inhibits the eukaryotic proteasome by a novel mechanism. *Nature*, 452, 755–758.
- Hardy, R. W., Holsten, R. D., Jackson, E. K., & Burns, R. C. (1968). The acetylene-ethylene assay for n(2) fixation: Laboratory and field evaluation. *Plant Physiology*, 43, 1185–1207.
- Hofstetter, S. S., Dudnik, A., Widmer, H., & Dudler, R. (2013). *Arabidopsis* yellow stripe-Like7 (YSL7) and YSL8 transporters mediate uptake of *Pseudomonas* virulence factor Syringolin A into plant cells. *Molecular Plant-Microbe Interactions*, 26, 1302–1311.
- Kakar, K., Wandrey, M., Czechowski, T., Gaertner, T., Scheible, W. R., Stitt, M., ... Udvardi, M. K. (2008). A community resource for high-throughput quantitative RT-PCR analysis of transcription factor gene expression in *Medicago truncatula*. *Plant Methods*, 4, 18.

- Kobayashi, T., & Nishizawa, N. K. (2012). Iron uptake, translocation, and regulation in higher plants. *Annual Review on Plant Biology*, *63*, 131–152.
- Kryvoruchko, I. S., Routray, P., Sinharoy, S., Torres-Jerez, I., Tejada-Jiménez, M., Finney, L. A., ... Udvardi, M. K. (2018). An iron-activated citrate transporter, MtMATE67, is required for symbiotic nitrogen fixation. *Plant Physiology*, *176*, 2315–2329.
- Kumar, R. K., Chu, H.-H., Abundis, C., Vasques, K., Rodriguez, D. C., Chia, J.-C., ... Walker, E. L. (2017). Iron-nicotianamine transporters are required for proper long distance iron signaling. *Plant Physiology*, *175*, 1254–1268.
- Kumar, S., Stecher, G., & Tamura, K. (2016). MEGA7: Molecular evolutionary genetics analysis version 7.0 for bigger datasets. *Molecular Biology and Evolution*, *33*, 1870–1874.
- Lubkowitz, M. (2011). The Oligopeptide transporters: A small gene family with a diverse group of substrates and functions? *Molecular Plant*, *4*, 407–415.
- Marschner, P. (2011). In P. Marschner (Ed.), *Mineral nutrition of higher plants* (3rd ed.). London, United Kingdom: Academic Press.
- Nakagawa, T., Kurose, T., Hino, T., Tanaka, K., Kawamukai, M., Niwa, Y., ... Kimura, T. (2007). Development of series of gateway binary vectors, pGWBs, for realizing efficient construction of fusion genes for plant transformation. *Journal of Bioscience and Bioengineering*, *104*, 34–41.
- Nozoye, T., Nagasaka, S., Kobayashi, T., Takahashi, M., Sato, Y., Sato, Y., ... Nishizawa, N. K. (2011). Phytosiderophore efflux transporters are crucial for iron acquisition in graminaceous plants. *Journal of Biological Chemistry*, *286*, 5446–5454.
- Olsen, L. I., & Palmgren, M. G. (2014). Many rivers to cross: The journey of zinc from soil to seed. *Frontiers in Plant Science*, *5*, 30.
- Osawa, H., Stacey, G., & Gassmann, W. (2006). ScOPT1 and AtOPT4 function as proton-coupled oligopeptide transporters with broad but distinct substrate specificities. *Biochemical Journal*, *393*, 267–275.
- Pilon, M. (2011). Moving copper in plants. *New Phytologist*, *192*, 305–307.
- Roberts, L. A., Pierson, A. J., Panaviene, Z., & Walker, E. L. (2004). Yellow Stripe1. Expanded roles for the maize iron-phytosiderophore transporter. *Plant Physiology*, *135*, 112–120.
- Schaaf, G., Ludewig, U., Erenoglu, B. E., Mori, S., Kitahara, T., & von Wiren, N. (2004). ZmYS1 functions as a proton-coupled symporter for phytosiderophore- and nicotianamine-chelated metals. *Journal of Biological Chemistry*, *279*, 9091–9096.
- Tadege, M., Wen, J., He, J., Tu, H., Kwak, Y., Eschstruth, A., ... Mysore, K. S. (2008). Large-scale insertional mutagenesis using the *Tnt1* retrotransposon in the model legume *Medicago truncatula*. *Plant Journal*, *54*, 335–347.
- Tejada-Jiménez, M., Castro-Rodríguez, R., Kryvoruchko, I., Lucas, M. M., Udvardi, M., Imperial, J., & González-Guerrero, M. (2015). *Medicago truncatula* natural resistance-associated macrophage Protein1 is required for iron uptake by rhizobia-infected nodule cells. *Plant Physiology*, *168*, 258–272.
- Tejada-Jiménez, M., Gil-Diez, P., Leon-Mediavilla, J., Wen, J., Mysore, K. S., Imperial, J., & Gonzalez-Guerrero, M. (2017). *Medicago truncatula* Molybdate transporter type 1 (MOT1.3) is a plasma membrane molybdenum transporter required for nitrogenase activity in root nodules under molybdenum deficiency. *New Phytologist*, *216*, 1223–1235.
- Terry, R. E., Soerensen, K. U., Jolley, V. D., & Brown, J. C. (1991). The role of active *Bradyrhizobium japonicum* in iron stress response of soybeans. *Plant and Soil*, *130*, 225–230.
- Vernoud, V., Journet, E. P., & Barker, D. G. (1999). MtENOD20, a nod factor-inducible molecular marker for root cortical cell activation. *Molecular Plant-Microbe Interactions*, *12*, 604–614.
- Waters, B. M., Chu, H.-H., DiDonato, R. J., Roberts, L. A., Easley, R. B., Lahner, B., ... Walker, E. L. (2006). Mutations in *Arabidopsis* Yellow Stripe-Like1 and Yellow Stripe-Like3 reveal their roles in metal ion homeostasis and loading of metal ions in seeds. *Plant Physiology*, *141*, 1446–1458.
- Winston, F., Dollard, C., & Ricupero-Hovasse, S. L. (1995). Construction of a set of convenient *Saccharomyces cerevisiae* strains that are isogenic to S288C. *Yeast*, *11*, 53–55.
- Yordem, B. K., Conte, S. S., Ma, J. F., Yokosho, K., Vasques, K. A., Gopalsamy, S. N., & Walker, E. L. (2011). *Brachypodium distachyon* as a new model system for understanding iron homeostasis in grasses: Phylogenetic and expression analysis of yellow stripe-like (YSL) transporters. *Annals of Botany*, *108*, 821–833.
- Zhao, H., & Eide, D. (1996). The ZRT2 gene encodes the low affinity zinc transporter in *Saccharomyces cerevisiae*. *Journal of Biological Chemistry*, *271*, 23203–23210.

SUPPORTING INFORMATION

Additional supporting information may be found online in the Supporting Information section at the end of this article.

How to cite this article: Castro-Rodríguez R, Escudero V, Reguera M, et al. *Medicago truncatula* Yellow Stripe-Like7 encodes a peptide transporter participating in symbiotic nitrogen fixation. *Plant Cell Environ*. 2021;44:1908–1920. <https://doi.org/10.1111/pce.14059>